CONVERSION OF ETHANOL OVER TRANSITION METAL OXIDE CATALYSTS: EFFECT OF TUNGSTA ADDITION ON CATALYTIC BEHAVIOR OF TITANIA AND ZIRCONIA

Thanh Khoa Phung[a], Loriana Proietti Hernández[a,b], Guido Busca[a]*

[a]Dipartimento di Ingegneria Civile, Chimica e Ambientale, Università di Genova, P.le J.F. Kennedy 1, I-16129, Genova, Italy

[b] on leave from Departamento de Termodinámica y Fenómenos de Transferencia, Universidad Simón Bolívar, AP 89000, Caracas 1080, Venezuela

* Tel: (+39) 010 353 6024, Fax: (+39) 010 353 6028, Email: Guido.Busca@unige.it (G. Busca)

Abstract

Ethanol dehydration was investigated (423 - 773 K, 1 atm, 1.43 h^{-1} WHSV in nitrogen) over titania, zirconia, as such and after impregnation with WO_3. As for comparison, data on other WO_3-free and WO_3-containing catalysts will be also discussed, considered a strong Lewis acid (alumina), a covalent oxide (silica) and a basic material (calcined hydrotalcite). The catalysts were characterized using FT-IR of adsorbed pyridine and of wolframate species, and by UV-Vis spectroscopy. The results presented here show that WO_3/ZrO_2 and WO_3/TiO_2 are excellent catalysts for ethanol dehydration. Their performances may compete with those of zeolites and alumina both for conversion to diethyl ether and to ethylene. The addition of WO_3 to both ZrO_2 and TiO_2 introduces strong Brønsted acid sites that are supposed to represent the active sites in the reaction, but also inhibits the formation of byproducts, i.e. acetaldehyde and higher hydrocarbons. This is attributed to the poisoning of basic sites and of reducible surface Ti and Zr centers, respectively.

Keywords: Ethanol dehydration; metal oxides; zirconia; titania; tungsten oxide, ethylene; diethyl ether; Lewis acidity; Brønsted acidity.

1 Introduction

Ethanol produced by fermentation of lignocellulosics, denoted as “second generation bioethanol”, could become a primary intermediate in the frame of a new industrial organic chemistry based on renewables [1,2].

Among the secondary intermediates potentially obtainable by converting (bio)ethanol, ethylene and diethyl ether can be obtained by catalytic dehydration

$$C_2H_5OH \rightarrow C_2H_4 + H_2O \qquad (1)$$

$$2\ C_2H_5OH \rightarrow C_2H_5OC_2H_5 + H_2O \qquad (2)$$

Reaction (1) has already been applied at the industrial level in the sixties using aluminas as the catalysts [3,4]. Different opinions exist on the potential practical improvement that can arise by the use of protonic zeolite catalysts instead of aluminas [5,6]. Both on alumina [7] and on some zeolites almost 100% yield to ethylene can be obtained at moderate temperature in lab scale experiments. Reaction (2) occurs on the same catalysts at moderate ethanol conversion, allowing very high selectivities and significant yields (> 70 %).

Also acetaldehyde can be obtained by ethanol, through dehydrogenation:

$$C_2H_5OH \rightarrow C_2H_4O + H_2 \qquad (3)$$

This reaction too has been used industrially in early times using either metal or zinc oxide catalysts [8]. Several other chemical intermediates can be obtained from ethanol, such as, e.g. acetic acid [9], ethyl acetate [10], higher olefins [11], isobutene [12], butadiene [13,14], and others.

The conversion of alcohols is also largely used as a test reaction for surface acido-basicity characterization [15,16,17,18]. Dehydration to olefins or ethers are typically observed on acid catalysts but the roles of Brønsted and Lewis acidity on these reactions and are still under discussion. Alcohol dehydrogenation to carbonyl compounds is instead assumed to occur on basic catalysts. However, as said for acetaldehyde synthesis, industrial alcohols dehydrogenations are carried out either on metal catalysts or on ZnO [19].

Metal oxides are characterized by Lewis type acidity and basicity as a function of the ionicity of the metal oxygen-bond and size and charge of the cation [20]. Brønsted acidity is observed on the oxides of high oxidation state elements. Among these elements, hexavalent tungsten is reported to give rise to stable very acidic catalytic materials active

in several acid-catalyzed processes, including alcohol dehydration reactions [21,22,23,24,25]. In particular tungsta-zirconias represent very interesting acid catalysts already developed at the industrial level for paraffin isomerization [26], but the reasons of their high activity has not been fully clarified [27,28].

In this paper results are reported on the catalytic activity of some metal oxides in ethanol conversion. In particular, the focus is on the addition of tungsten oxide to transition metal oxide catalysis, i.e. zirconia and titania. As for comparison, data on other WO_3-free and WO_3-containing catalysts will be also discussed, considered a strong Lewis acid (alumina), a covalent oxide (silica) and a basic material (calcined hydrotalcite). The aim of this work is to go deeper on the mechanisms of ethanol conversion reactions over different Brønsted and Lewis acido-basic solids, and on the catalytic activity/surface structure/bulk structure relationships for metal oxide systems.

2 Experimental.

2.1. Catalysts

The catalysts properties are summarized in Tables 1. ZrO_2 was precipitated from $Zr(NO_3)_4$ (MEL Chemicals, solution 40 %) [29]. The preparation of tungsten-supported catalysts was accomplished by impregnating the supports with an aqueous solution containing $5(NH_4)_2O.12WO_3.5H_2O$ from Carlo Erba, followed by drying and calcining for 3 h at 673 K. The composition of the catalysts is 13.6% (wt/wt) WO_3 / support, as in the commercial WO_3/TiO_2 sample, also considered in the paper.

2.2. Catalytic experiments

Catalytic experiments were performed at atmospheric pressure in a tubular flow reactor (i.d. 6 mm) using 0.5 g catalyst (60-70 mesh sieved, to have a ratio between the particle diameter and the internal reactor diameter near 25) and feeding 7.9% v/v ethanol in nitrogen with 1.43 h^{-1} WHSV (total flow rate of 80 cc/min). The carrier gas (nitrogen) was passed through a bubbler containing ethanol (96%) maintained at constant temperature (298 K) in order to obtain the desired partial pressures. The temperature in the experiment was varied stepwise from 423 K to 773 K.

Ethanol conversion is defined as usual:

$$X_{EtOH} = (n_{EtOH(in)} - n_{EtOH(out)})/n_{EtOH(in)}$$

While selectivity to product *i* is defined as follows:

$S_i = n_i/(\nu_i(n_{EtOH(in)} - n_{EtOH(out)}))$

where n_i is the moles number of compound *i*, and ν_i is the ratio of stoichiometric reaction coefficients.

The outlet gases were analyzed by a gas chromatograph (GC) Agilent 4890 equipped with a Varian capillary column "Molsieve 5A/Porabond A Tandem" and TCD and FID detectors in series. In order to identify the compounds of the outlet gases, a gas chromatography coupled with mass spectroscopy (GC-MS) Thermo Scientific with TG-SQC column (15 m x 0.25 mm x 0.25 μm) was used.

2.3. Catalyst characterization:

UV-Vis analysis has been performed using a Jasco V570 instrument, equipped with a DR integration sphere for the analysis of fresh and spent catalysts powder. All the spectra have been recorded in air at room temperature.

Acidity measurements were done using the pure powders pressed into thin wafers and activated in the IR cell connected with a conventional outgassing/gas-manipulation apparatus at 773 K. The activated samples were contacted with pyridine vapor (p_{Py} ~1 torr) at room temperature for 15 min; after which the IR spectra of the surface species were collected in continuous evacuation at room temperature with increasing temperature.

3 Results.

3.1. UV-Vis study

The diffuse reflectance UV-Vis spectra, recorded in air, of the fresh catalysts are presented in the Fig. 1. In case of ZrO_2 the inflection point of the absorption edge is near 240 nm due to $O^{2-} \rightarrow Zr^{4+}$ charge transfer transitions, corresponding to the excitation of electrons from the valence band (having O 2p character) to the conduction band (having Zr 4d character) [30]. For titania the absorption edge is stronger, near 380 nm, due to charge transfer transition from valence band (having mainly O 2p character) to the conduction band (having Ti 3d character) [31,32].

The WO_3-containing samples all show absorption in the UV region due to the $O^{2-} \rightarrow W^{6+}$ charge transfer transition corresponding to the transition of electrons from the O 2p valence band to the W 5d levels. Indeed, WO_3 does not modify the spectra of TiO_2, this is because the empty orbitals of hexavalent tungsten (W 5d) lie into the Ti 3d conduction band so that the $O^{2-} \rightarrow W^{6+}$ charge transfer transition are superimposed to or, more likely, mixed with the $O^{2-} \rightarrow Ti^{4+}$ charge transfer transition [30]. In case of WO_3/ZrO_2, addition of

WO_3 modifies the UV-Vis spectrum of ZrO_2, due to the lower energy of the W 5d levels with respect to the Zr 4d conduction band. In the cases of WO_3/SiO_2 and $WO_3/MgO\text{-}Al_2O_3$ the absorption in the UV-Vis is also observed, but weaker and broader. On SiO_2, the addition of WO_3 results in an increased absorption with a broad edge near 380 nm. The spectrum observed in the case of $WO_3/MgO\text{-}Al_2O_3$ shows a broad weak absorption, which could be consistent with the formation of $MgWO_4$ domains [33].

3.2 IR spectra of activated samples.

The IR spectra of titania and zirconia pressed disks with and without the addition of WO_3, recorded after activation by outgassing at 773 K, are reported in Fig. 2. The spectra of the two single oxides show a band in the region 1400-1350 cm^{-1} which is typical of sulphate species in a "monoxo" form [34]. The band is found at 1368 cm^{-1} on titania, with a tail at lower frequencies, and is split into two components at 1360 and 1348 cm^{-1} on zirconia. This shows in both cases some heterogeneity of such sulphate species. On both WO_3-containing samples an additional band which can be assigned to tungstate species is found near 1010 cm^{-1}, which is typical for monoxo-tungstate species [25,30,35]. In the case of the WO_3/TiO_2 (H) sample the band of sulphate species is fully disappeared, suggesting that the addition of tungstate destabilized sulphate species that are decomposed during the later calcination. In the case of the WO_3/ZrO_2 sample, instead, the band of sulphate species is still present, now single and shifted upwards (1386 cm^{-1}).

The spectrum of the $MgO\text{-}Al_2O_3$ sample, instead (Fig. 3), shows (even after outgassing) a very strong band extending from ca. 1600 to 1350 cm^{-1}, typically due to carbonate species. This agrees with the strong basic nature of this oxide and the difficulty in desorbing carbonate species [36]. The addition of WO_3 to $MgO\text{-}Al_2O_3$ causes the strong decrease of the bands of carbonates and the appearance of a new band at 863 cm^{-1} which is consistent for the highest W=O stretching mode of polymeric wolframate species of the wolframite type [37], showing a strong interaction of wolframate with magnesium giving rise to $MgWO_4$-like structure.

3.3. Surface acidity characterization by IR spectroscopy of adsorption of pyridine.

The surface acidity of investigated catalysts has been characterized by IR spectroscopy of pyridine adsorption (Fig. 4). The main bands of adsorbed species on TiO_2 and ZrO_2 are observed at ca. 1602-1610, 1575, 1489 and 1445 cm^{-1} due to the 8a, 8b, 19a and 19b

modes of molecular pyridine bonded to medium-strong Lewis acid sites [38]. After addition of WO_3 on TiO_2 and ZrO_2, the bands of Lewis-bonded pyridine after outgassing at 323 K are slightly shifted upwards, likely due to a slightly increased strength of the Lewis acid sites, or of new Lewis sites associated to tungsten ions. In any case, the strength of Lewis sites on these samples, as measured by the position of the bands of adsorbed pyridine, is far lower than that of alumina taken as a reference (bands at 1622 and 1615 cm^{-1}, 8a, and at ca. 1460 cm^{-1}, 19b [7]). Additionally, two new bands appear at 1639 and 1536-1541 cm^{-1}, which are associated to pyridinium ions 8a and 19a modes [39], respectively. This provides evidence of the presence of both Lewis and Brønsted acid sites on both WO_3/TiO_2 (H) and WO_3/ZrO_2 samples.

Interestingly, while $MgO\text{-}Al_2O_3$ does not show the presence of adsorbed pyridine after outgassing at 323 K (in agreement with its low acidity and strong basicity), on $WO_3/MgO\text{-}Al_2O_3$ Lewis-bonded but no Brønsted-bonded pyridine is found. This confirms that the state of tungsten oxide species is different when deposited on $WO_3/MgO\text{-}Al_2O_3$ than on titania and zirconia, as also shown by IR and UV experiments, and that tungsten oxide species may provide either Lewis or Brønsted acidity or even both, as discussed previously [30].

3.4. Catalytic conversion of ethanol (EtOH)

Ethanol conversion and selectivity to C-containing products observed over the catalysts investigated here are reported in Tables 2 and 3. The evaluation of the activation energies for ethanol conversions (all above 80 kJ/mol) indicate that, at least on low temperature-low conversion conditions, diffusional limitations are not significant.

The trend of conversion of ethanol (Fig. 5) over the metal oxides is $Al_2O_3 > TiO_2 > ZrO_2 > MgO\text{-}Al_2O_3 > SiO_2$. This trend can be roughly related to the strength of the Lewis acid sites observed by IR experiments of pyridine adsorption and to the polarizing power of the cations expressed as charge/radius: 7.7 for tetrahedral Al^{3+} of alumina > 6.6 for octahedral Ti^{4+} of anatase > ~ 5.0 for Zr^{4+} in coordination eight in tetragonal zirconia > 3.7 of tetrahedral Mg^{2+} in $MgAl_2O_4$ > 0 for covalently bonded silicon in silica [20]. $\gamma\text{-}Al_2O_3$, whose behaviour has been discussed previously [7] and that is considered here as a reference catalyst, shows strongest Lewis acidity and conversion, highest selectivity to diethyl ether at low conversion and to ethylene at high conversion, small amounts of other products being observed only at almost total conversion (2 % ethane + C_4 hydrocarbons). On ZrO_2, although high yields of ethylene are obtained (87 % at 773 K), a number of other

compounds are produced among which acetaldehyde at low conversion, and C_2 (ethane)-C_{5+} hydrocarbons and CO_2 at high conversion. Titania is more active than zirconia in converting ethanol, but even less selective to ethylene, mainly due to the even higher production, in particular, of C_4 hydrocarbons (ca. 40 % yield at 673 K). Over MgO-Al_2O_3, considered here as a reference of a strongly basic catalyst, diethyl ether and ethylene are still the main products, although acetaldehyde is produced with higher selectivities and yields with respect to the other oxides. In this case also interesting production of other carbonyl compounds is found, likely due to aldol-like conversion of acetaldehyde. The catalytic activity of silica is the lowest, although conversion obtained is still higher than that obtained on silica-glass, a low surface area material used as an “inert” filling material for the “empty” reactor, to evaluate the extent of “non catalytic” reaction. Thus, also silica gives rise to a weak catalytic activity producing again ethylene and diethyl ether as the main products, but also 10 % selectivity to acetaldehyde.

In Fig. 5 the effect of WO_3 on ethanol conversion on titania and zirconia is also shown. As the result of the addition of WO_3 oxide, the catalytic activity of zirconia and titania increases significantly. Interestingly, addition of WO_3 makes these catalysts more selective to diethyl ether at low conversion and to ethylene at high conversion. In practice, the activity producing not only acetaldehyde but also other hydrocarbons (ethane, C_3-C_{5+}) is strongly depressed by addition of WO_3 on both zirconia and titania. WO_3/ZrO_2 and home-made WO_3/TiO_2 (H) are the best catalysts (among those studied here) for ethylene production with 98.3-99.0 % yield at 623 K. Thus these materials are actually more active than alumina in converting ethanol but can finally have very similar best performances as ethanol dehydration catalysts to produce ethylene as alumina.

In the case of the two WO_3/TiO_2 samples, the ethanol conversion of commercial mixed oxide WO_3/TiO_2 (C) is higher than home-made mixed oxide WO_3/TiO_2 (H) possibly due to the effect of the higher surface area. However, the selectivity to ethylene of the commercial powder is lower, mainly because of oligomerization reaction of ethylene to higher hydrocarbons in comparison to home-made mixed oxide catalyst. On the other hand, the commercial WO_3/TiO_2 (C) powder gives excellent results in producing diethyl ether (73 % yield at 473 K) which is only slightly lower with respect to that obtained, in the same conditions, on zeolites (74.6 % yield to diethyl ether at 473 K on H-BEA [40]).

WO_3/SiO_2 is, in contrast to pure silica, quite an active catalyst at low temperature. Its activity is definitely lower than that of WO_3/TiO_2 and WO_3/ZrO_2, but comparable to that of

alumina at low temperature. Only in the case of $MgO-Al_2O_3$ the addition of WO_3 does not increase catalytic activity in ethanol conversion.

3.1. UV-Vis study of spent TiO_2, ZrO_2, WO_3/TiO_2 and WO_3/ZrO_2 catalysts.

The diffuse reflectance UV-Vis spectra, recorded in air, of spent TiO_2, ZrO_2 and their corresponding WO_3-containing catalysts, recorded after the full catalytic run up to 773 K, are presented in the Fig. 6. In the case of TiO_2, the O 2p → Ti 3d edge of the fresh catalyst is totally lost, while an almost continuous absorption appears centered mainly in the visible region in agreement with the dark color of the sample. The absence of definite components in the UV-vis spectrum suggests that this absorption is not due to carbonaceous species, but to the reduction of the catalyst to a TiO_{2-x} bulk. In contrast, spent ZrO_2 (grey colour) still shows the sharp O 2p → Zr 4d edge of fresh ZrO_2, near 240 nm, with very weak absorption in the visible region.

Looking at their WO_3-containing catalysts, the situation is reversed. In the case of WO_3/ZrO_2 catalysts, the spectrum of the fresh catalyst is totally lost, showing now a continuous absorption centered mainly in the visible region. This shows that this catalyst works in a highly reduced state. In contrast, the spectra of the two spent WO_3/TiO_2 catalysts still show the titania absorption edge, near 380 nm. The edge is actually decreased in intensity with respect to the fresh catalysts, while a broad absorption is formed in the visible region in particular in the case of the commercial sample. The spectra indicate that the WO_3/TiO_2 catalysts work in a only slightly reduced state.

A interpretation for this behaviour may be attempted on the basis of the information, arising from the spectra of the fresh catalysts (Fig. 1), that the W 5d levels of surface WOx species lie well below the Zr 4d of zirconia, but above the Ti 3d levels of titania. Thus, surface tungsten species might “protect” the titania surface from reduction while favours reduction of zirconia.

Discussion

The data reported here show that zirconia and titania have moderately high activity in converting ethanol to ethylene and diethyl ether. Their catalytic activity is attributed to the moderately high Lewis acidity of Ti^{4+} and Zr^{4+} sites, that activates ethoxy groups, the intermediates for this reaction as discussed previously for alumina catalysts [7]. However, on zirconia and titania selectivity to diethyl ether and ethylene is lowered by the production

of acetaldehyde at low temperature and by the formation of higher hydrocarbons at high temperature. The formation of acetaldehyde may be attributed to some basicity of these materials, as usually done and as found here for the basic material denoted as $MgO\text{-}Al_2O_3$. The formation of higher hydrocarbons, which is very important on titania and only to a lower extent on zirconia, is not easily assigned. We tentatively correlate this catalytic activity to the slight surface reducibility of these oxides. It is in fact well-known that both titania and zirconia may give rise to very slight surface reduction producing reduced centers such as Ti^{3+} and Zr^{3+}. It is also well-known that partially reduced Ti and Zr centers are active in olefin polymerization reactions, being the active centers in Ziegler Natta catalysts such as those based on $TiCl_3$ [41] and those based on metallocenes [42]. It is possible to associate t to the overconversion of ethylene to oligomers, that can also give rise to hydrogenation/dehydrogenation sites producing both olefins and paraffins. In fact, the products of this reactivity are always found in conditions where production of ethylene is already fast.

The addition of tungsten oxide changes very much the situation. In fact, WO_3/TiO_2 and WO_3/ZrO_2 are both much more active in converting ethanol to diethyl ether at low temperature and conversion, and to ethylene at high temperature and conversion. This higher activity is certainly associated to the Brønsted acidity of the W-OH bonds, for which evidence is provided by pyridine adsorption. In parallel, the suppression of dehydrogenation activity to acetaldehyde is likely associated to the “poisoning” of basic sites of the pure oxides. In fact, the acidic species WO_x certainly interact with and poison the basic sites of the supports.

In particular in the case of TiO_2, the addition of WO_3 results also in the disappearance of the production of higher hydrocarbons, previously attributed to the overconversion of ethylene by reduced metal centers. In fact, UV-vis spectra show that surface WO_3 oxide protects TiO_2 surface from reduction, thus reducing the amount of reduced Ti surface sites active in overconverting ethylene. According to this approach, the commercial WO_3/TiO_2 (C) catalyst works more reduced than the home made WO_3/TiO_2 (H) catalyst, and is also less selective to ethylene at high temperature with higher residual formation of higher hydrocarbons. This may be also associated to the higher surface area of WO_3/TiO_2 (C) catalyst, whose surface coverage by the same amount of WO_3 is obviously lower.

The UV-Vis spectra, show that spent WO_3/ZrO_2 works in a deeply reduced state, as already reported for similar catalysts in hydrocarbon conversions [27,43]. Although the

ability of WO_3/ZrO_2 to reduce quite extensively can be a good property in paraffin oligomerization, where dehydrogenation/rehydrogenation steps could occur in series to Brønsted acid-catalyzed steps, this is probably not needed in ethanol dehydration, where in fact the least reduced catalyst WO_3/TiO_2 appear to be more active than the deeply reducible WO_3/ZrO_2 catalyst. It seems that reducibility does not result in stronger acidity and activity.

4 Conclusions.

The results presented here show that WO_3/ZrO_2 and WO_3/TiO_2 are excellent catalysts for ethanol dehydration. Their performances may compete with those of zeolites and alumina for conversion to both diethyl ether and to ethylene. The addition of WO_3 to both ZrO_2 and TiO_2 introduces strong Brønsted acid sites that are supposed to represent the active sites in the reaction, but also inhibits the formation of byproducts, i.e. acetaldehyde and higher hydrocarbons. This is attributed to the poisoning of basic sites and of reducible surface Ti and Zr centers, respectively by WO_3 species. Although WO_3/ZrO_2 and, to a lower extent, also WO_3/TiO_2 work in an at least partially reduced state, it does not seem that reducibility is needed for generation of strong Brønsted acdidity.

Acknowledgements

TKP acknowledges funding by EMMA in the framework of the EU Erasmus Mundus Action 2.

Table 1. The properties of investigated catalysts

Notation	Commercial name and composition	Manufacturer	Preparation	Crystal phase	S_{BET}
$MgO-Al_2O_3$	Pural MG70 (Mg:Al 70:30)	Sasol	Calcined at 773 K for 4h	Amorphous	-
SiO_2	Silica Gel SG127	Grace Davison	as received	Amorphous	-
ZrO_2	-	-	Precipated from Zr nitrate at 723 K	Monoclinic	94
TiO_2	Titania	Rhône-Poulenc	as received	Anatase	70
Al_2O_3	Puralox SBa 200	Sasol	From boehmite via Al alkoxides	Gamma	190±10
$WO_3/MgO-Al_2O_3$	13.6% (wt/wt) WO_3 Mg:Al 70:30	Home-made	Impregnated, dried and calcined at 673 K for 3h	Amorphous	-
WO_3/SiO_2	13.6% (wt/wt) WO_3 -	Home-made	Impregnated, dried and calcined at 673 K for 3h	Amorphous	
WO_3/ZrO_2	13.6% (wt/wt) WO_3	Home-made	Impregnated, dried and calcined at 673 K for 3h	Monoclinic	81±10
WO_3/TiO_2 (H)	13.6% (wt/wt) WO_3 -	Home-made	Impregnated, dried and calcined at 673 K for 3h	Anatase	60±10
WO_3/TiO_2 (C)	Titan A-DW-1 13.6% (wt/wt) WO_3	Bayer	as received	Anatase	80

Table 2. Conversion (on C-basis) and selectivity (S) to C-containing products of ethanol as a function of reaction temperature.

Catalyst	Temp.	TC	C_2H_4	C_2H_6	CH_3CHO	C_4	DEE	Others
SiO_2	423	0.0	-	-	-	-	-	-
	473	0.0	-	-	-	-	-	-
	523	0.2	0.0	0.0	0.0	0.0	100.0	0.0
	573	0.6	24.6	0.0	0.0	0.0	75.4	0.0
	623	2.5	35.5	0.0	9.1	0.0	55.5	0.0
	673	8.6	48.8	9.2	9.4	0.0	31.8	0.8
	723	15.0	72.5	5.4	9.0	1.9	8.5	2.7
	773	33.4	81.0	4.4	9.2	1.7	1.3	2.4
$MgO\text{-}Al_2O_3$	423	0.0	-	-	-	-	-	-
	473	0.1	0.0	0.0	0.0	0.0	100.0	0.0
	523	0.9	5.2	0.0	25.4	0.0	61.6	7.8
	573	3.4	15.6	0.0	14.0	0.0	50.6	19.8
	623	11.2	41.3	0.0	23.8	6.1	20.1	8.7
	673	28.5	53.3	0.0	26.2	9.3	7.4	3.8
	723	65.8	56.4	0.1	15.9	14.7	2.3	10.6
	773	100.0	51.7	0.9	1.1	11.2	1.3	33.8
ZrO_2	423	0.0	-	-	-	-	-	-
	473	0.0	-	-	-	-	-	-
	523	0.4	43.2	0.0	0.0	0.0	56.8	0.0
	573	5.6	73.4	0.0	14.8	3.0	8.8	0.0
	623	45.4	79.3	0.0	4.5	6.8	3.2	6.2
	673	100.0	75.4	0.0	0.0	3.5	1.5	19.6
	723	100.0	82.7	0.0	0.0	1.2	0.2	15.9
	773	100.0	87.3	0.0	0.0	0.4	0.1	12.2
TiO_2	423	0.0	-	-	-	-	-	-
	473	0.6	0.0	0.0	16.2	0.0	83.8	0.0
	523	8.8	12.7	0.0	4.4	0.0	82.9	0.0
	573	37.7	17.1	1.3	3.2	2.8	75.6	0.0
	623	80.1	14.1	6.8	2.5	16.6	59.4	0.6
	673	100.0	29.7	23.3	0.0	39.9	0.0	7.1
	723	100.0	47.9	23.2	0.0	18.5	0.0	10.4
	773	100.0	65.1	7.7	10.4	0.0	0.0	16.8
Al_2O_3	423	0.3	0.0	0.0	0.0	0.0	100.0	0.0
	473	20.8	0.9	0.0	0.0	0.0	99.1	0.0
	523	77.8	20.1	0.1	0.0	0.1	79.6	0.1
	573	99.7	97.4	0.3	0.0	2.0	0.3	0.0
	623	100.0	98.4	0.6	0.0	1.0	0.0	0.0
	673	100.0	98.9	0.3	0.0	0.6	0.0	0.2
	723	100.0	99.0	0.5	0.0	0.3	0.0	0.2
	773	100.0	98.8	0.7	0.0	0.2	0.0	0.3
WO_3/SiO_2	423	1.2	0.0	0.0	0.0	0.0	100.0	0.0

	473	10.2	26.3	0.0	0.0	0.0	73.7	0.0
	523	37.2	54.4	0.0	0.4	0.0	45.2	0.0
	573	54.8	77.7	0.4	0.6	0.0	21.3	0.0
	623	74.8	91.8	0.9	1.0	0.0	6.0	0.3
	673	94.4	92.6	1.8	2.0	0.6	2.2	0.8
	723	100.0	92.0	1.9	3.4	0.7	0.8	1.2
	773	100.0	92.6	1.6	4.1	0.3	0.3	1.1
$WO_3/MgO\text{-}Al_2O_3$	423	0.0	-	-	-	-	-	-
	473	0.0	-	-	-	-	-	-
	523	0.4	0.0	0.0	0.0	0.0	100.0	0.0
	573	3.7	16.7	0.0	15.2	0.0	60.1	8.0
	623	7.2	31.3	0.0	20.4	4.1	41.7	2.5
	673	30.3	41.0	1.7	21.8	13.5	17.6	4.4
	723	79.9	45.7	2.0	12.2	23.6	4.5	12.0
	773	100.0	42.2	2.7	1.5	22.2	2.0	29.4
WO_3/ZrO_2	423	0.5	0.0	0.0	0.0	0.0	100.0	0.0
	473	8.7	6.2	0.0	0.0	0.0	93.8	0.0
	523	53.9	21.3	0.0	0.3	0.0	78.3	0.1
	573	97.5	94.0	0.2	0.6	0.8	4.2	0.2
	623	100.0	99.0	0.4	0.2	0.1	0.0	0.3
	673	100.0	98.6	0.6	0.1	0.3	0.0	0.4
	723	100.0	95.0	2.7	0.1	0.8	0.0	1.4
	773	100.0	90.5	5.3	0.1	1.2	0.0	2.9
WO_3/TiO_2 (H)	423	12.2	0.0	0.0	0.0	0.0	100.0	0.0
	473	70.4	4.1	0.0	0.0	0.0	95.9	0.0
	523	88.6	54.6	0.0	0.4	0.0	44.9	0.1
	573	100.0	96.8	0.9	0.6	0.9	0.5	0.3
	623	100.0	98.3	1.6	0.0	0.0	0.0	0.1
	673	100.0	95.9	3.4	0.0	0.4	0.0	0.3
	723	100.0	92.4	5.4	0.2	0.8	0.0	1.2
	773	100.0	90.0	7.2	0.5	0.8	0.0	1.5
WO_3/TiO_2 (C)	423	27.7	1.4	0.0	0.0	0.0	98.6	0.0
	473	87.3	15.9	0.0	0.3	0.0	83.9	0.0
	523	100.0	92.7	0.0	0.0	4.9	0.0	2.4
	573	100.0	44.6	9.2	0.0	31.1	0.0	15.1
	623	100.0	59.0	10.3	0.0	21.9	0.0	8.8
	673	100.0	66.6	18.0	0.0	9.4	0.0	6.0
	723	100.0	71.4	19.1	0.0	3.1	0.0	6.4
	773	100.0	72.5	19.1	0.0	0.8	0.0	7.6

Table 3. Selectivity (S) to C-containing products of others products in Table 2 as a function of reaction temperature.

Catalyst	Temp.	TC	% Others	Others			
				SCO_2 (%)	C_3 (%)	Acetone + ketone (%)	C_{5+} (%)
$MgO-Al_2O_3$	523	0.9	7.8	100.0	0.0	0.0	0.0
	573	3.4	19.8	100.0	0.0	0.0	0.0
	623	11.2	8.7	87.5	12.5	0.0	0.0
	673	28.5	3.8	48.7	21.6	29.7	0.0
	723	65.8	10.6	36.2	12.4	28.6	13.0
	773	100.0	33.8	24.2	8.3	36.0	7.9
ZrO_2	623	45.4	6.2	36.1	14.8	0.0	49.2
	673	100.0	19.6	22.4	37.2	0.0	40.3
	723	100.0	15.9	24.4	46.3	0.0	25.0
	773	100.0	12.2	32.5	45.5	0.0	10.6
TiO_2	673	100.0	7.1	0.0	25.4	0.0	74.7
	723	100.0	10.4	0.0	22.9	0.0	64.8
	773	100.0	16.8	14.3	7.7	0.0	76.8
$WO_3/MgO-Al_2O_3$	573	3.7	8	100.0	0.0	0.0	0.0
	623	7.2	2.5	70.8	29.2	0.0	0.0
	673	30.3	4.4	22.2	8.9	5.2	59.3
	723	79.9	12	14.2	14.2	5.2	56.6
	773	100.0	29.4	14.6	11.5	36.0	33.1
WO_3/TiO_2 (C)	523	100.0	2.4	0.0	58.3	0.0	41.7
	573	100.0	15.1	0.0	11.3	0.0	87.9
	623	100.0	8.8	0.0	20.7	0.0	73.0
	673	100.0	6	0.0	33.9	0.0	38.9
	723	100.0	6.4	15.6	28.1	0.0	10.5
	773	100.0	7.6	23.7	18.4	0.0	0.0

Figure Captions

Figure 1. UV-Vis spectra of fresh catalysts.

Figure 2. FT-IR spectra of pure powder pressed disks of TiO_2, ZrO_2, WO_3/TiO_2 and WO_3/ZrO_2 after outgassing at 773 K.

Figure 3. FT-IR spectra of pure powder pressed disks of $MgO\text{-}Al_2O_3$ (calcined hydrotalcinte) and of $WO_3/MgO\text{-}Al_2O_3$ after outgassing at 773 K.

Figure 4. FT-IR subtraction spectra of surface species arising from pyridine adsorbed on investigated catalysts.

Figure 5. Catalytic conversion of ethanol over the investigated catalysts**.**

Figure 6. UV-Vis spectra of spent TiO_2, ZrO_2 and their WO_3-supported after catalytic run at 773 K.

References

[1] A. Limayem, S.C. Ricke, Prog. Energy Combust. Sci. 38 (2012) 449-467.

[2] M. Balat, Energy Convers. Manag. 52 (2011) 858-875.

[3] Y.C. Hu, in: J.J. McKetta (Ed.), Chemical Processing Handbook, Dekker, New York, 1993, p. 768.

[4] Ethylene from Ethanol, Chematur Engineering Group http://www.chematur.se/sok/download/Ethylene_rev_0904.pdf (20.05.2013)

[5] M. Zhang and Y. Yu, Ind. Eng. Chem. Res. 52 (2013) 9505-9514. DOI: 10.1021/ie401157c

[6] D. Fan, D.-J. Dai, H.-S. Wu, Mater. 6 (2013) 101-115. doi:10.3390/ma6010101

[7] T.K. Phung, A. Lagazzo, M.Á. Rivero Crespo, V. Sanchez Escribano, G. Busca, J. Catal. 311 (2014) 102-113.

[8] K. Weissermel, H.-J. Arpe Industrial Organic Chemistry, 4th ed., Weinheim : Wiley-VCH, 2008, p. 167.

[9] X. Li, E. Iglesia, Chem. Eur. J. 13 (2007) 9324 – 9330.

[10] S.W. Colley, C.R. Fawcett, M. Sharich, M. Tuck, D.J. Watson, M.A. Wood, United States Patent, US 7,553,397, B1 (2009).

[11] M. Inaba, K. Murata, M. Saito, I. Takahara, Green Chem., 9 (2007) 638-646.

[12] J. Sun, K. Zhu, F. Gao, C. Wang, J. Liu, C.H.F. Peden, Y. Wang, J. Am. Chem. Soc., 133 (29) (2011) 11096–11099. doi: 10.1021/ja204235v

[13] C. Angelici, B.M. Weckhuysen, P.C. Bruijnincx, ChemSusChem. 6 (2013) 1595-614.

[14] E.V. Makshina, M. Dusselier, W. Janssens, J. Degrève, P.A. Jacobs, B.F. Sels, Chem Soc Rev. (2014) Advance Article. DOI: 10.1039/c4cs00105b

[15] J.H. Kwak, D. Mei, C.H.F. Peden, R. Rousseau, J. Szanyi, Catal. Lett. 141 (2011) 649-655.

[16] S. Roy, G. Mpourmpakis, D.-Y Hong, D.G. Vlachos, A. Bhan, R.J. Gorte, ACS Catal. 2 (2012) 1846-1853.

[17] J.F. DeWilde, H. Chiang, D.A. Hickman, C.R. Ho, A. Bhan, ACS Catal. 3 (2013) 798-807.

[18] M. Caillot, A. Chaumonnot, M. Digne, J.A. Van Bokhoven, ChemCatChem. 6 (2014) 832-841.

[19] G. Busca, Heterogeneous Catalytic Materials, Elsevier, 2014, pp. 352-353.

[20] G. Busca, Chem. Phy. Phys. Chem. 1 (1999) 723-736.

[21] D. Varisli, T. Dogu, G. Dogu, Ind. Eng. Chem. Res. 48 (21) (2009) 9394–9401.

[22] D. Varisli, T. Dogu, G. Dogu, Chem. Eng. Sci. 65 (2010) 153-159.

[23] J. Macht, C.D. Baertsch, M. May-Lozano, S.L. Soled, Y. Wang, E. Iglesia, J. Catal. 227 (2004) 479–491.

[24] R. Ladera, E. Finocchio, S. Rojas, G. Busca, J.L.G. Fierro, M. Ojeda, Fuel. 113 (2013) 1–9.

[25] M. Massa, A. Andersson, E. Finocchio, G. Busca, J. Catal. 307 (2013) 170–184.

[26] G. Busca, Heterogeneous Catalytic Materials, Elsevier, 2014, pp. 173-174.

[27] C.D. Baertsch, K.T. Komala, Y.-H.Chua, E.Iglesia, J. Catal 205 (2002) 44-57.

[28] W. Zhou, E.I. Ross-Medgaarden, W.V. Knowles, M.S. Wong, I.E. Wachs, C.J. Kiely, . Nature Chem. 1 (2009) 722-728.

[29] M. Daturi, A. Cremona, F. Milella, G. Busca, E. Vogna, J. Eur. Ceram. Soc. 18 (1998) 1079-1087.

[30] A. Gutiérrez-Alejandre, P. Castillo, J. Ramírez, G. Ramis, G. Busca, Appl. Catal. A Gen. 216 (2001) 181-194.

[31] E. Fernández López, V. Sánchez Escribano, M. Panizza, M.M. Carnasciali, G. Busca, J. Mater. Chem. 11 (2001) 1891

[32] A. Kitiyanan, S. Sakulkhaemaruethai, Y. Suzuki, s. Yoshikawa, Compos. Sci. Technol. 66 (2006) 1259

[33] S. Dey, R.A. Ricciardo, H.L. Cuthbert, P.M. Woodward, Inorg Chem. 53(9) (2014) 4394-4399.

[34] O. Saur, M. Bensitel, A.B. Mohammed Saad, J.C. Lavalley, C.P. Tripp, B.A. Morrow, J. Catal. 99 (1986) 104.

[35] G. Busca, J. Raman Spectrosc. 33 (2002) 348-358.

[36] G. Busca, Chem. Rev. 110 (2010) 2217-2249.

[37] M. Daturi, G. Busca, M.M. Borel, A. Leclaire and P. Piaggio, J. Phys. Chem. 101 B (1997) 4358-4369.

[38] G. Busca, Catal. Today 41 (1998) 191-206.

[39] M. Castellà-Ventura, Y. Akacem, E. Kassab, J. Phys. Chem. C 112 (2008) 19045-19054.

[40] Unpublished results from our laboratory

[41] A. Correa, R. Credendino, J.T.M. Pater, G. Morini, L. Cavallo, Macromolecules, 45 (2012) 3695-3701.

[42] W. Kaminsky, Advan. Catal., 46 (2001) 89-159.

[43] S. Kuba, M.Che, R.K. Grasselli, H. Knözinger, J Phys. Chem. B 107 (2003) 3459-3463.

Figure 1

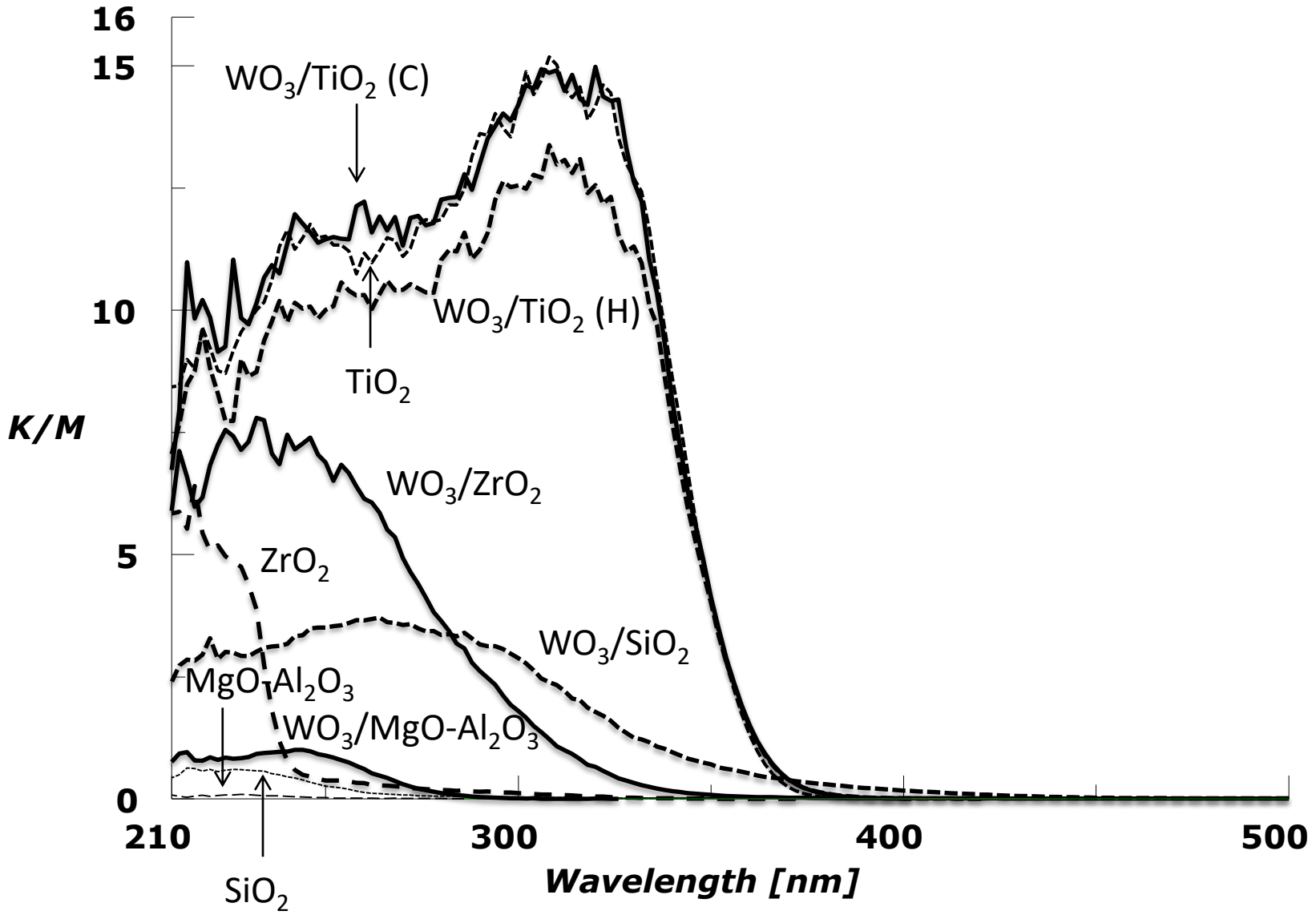
16
15
10
5
0
K/M
210
300
400
500
Wavelength [nm]
WO3/TiO2 (C)
WO3/TiO2 (H)
TiO2
WO3/ZrO2
ZrO2
WO3/SiO2
MgO-Al2O3
WO3/MgO-Al2O3
SiO2

Figure 2.

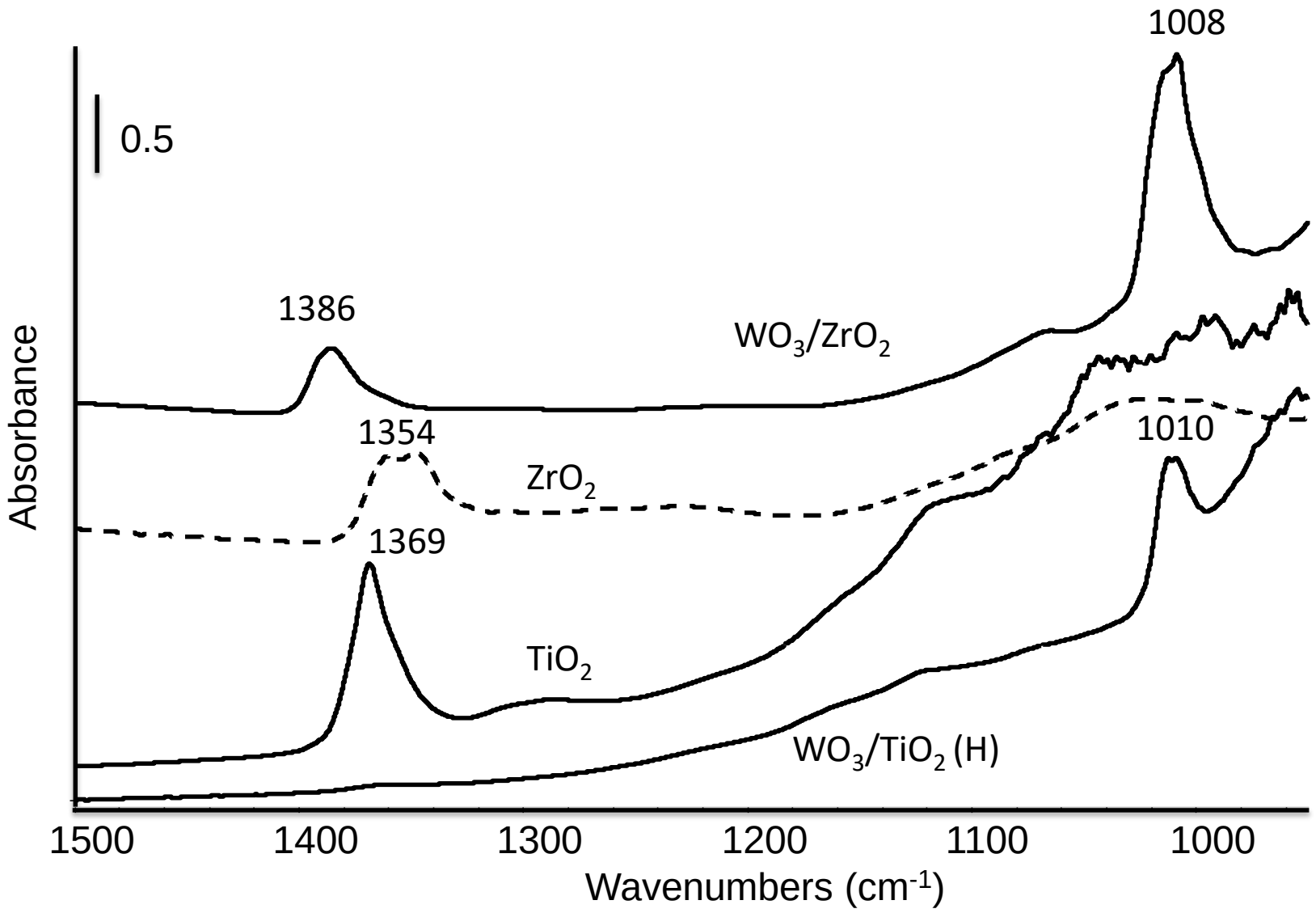
1008
0.5
1386
WO3/ZrO2
1354
ZrO2
1010
1369
TiO2
WO3/TiO2 (H)
Absorbance
1500
1400
1300
1200
1100
1000
Wavenumbers (cm-1)

Figure 3.

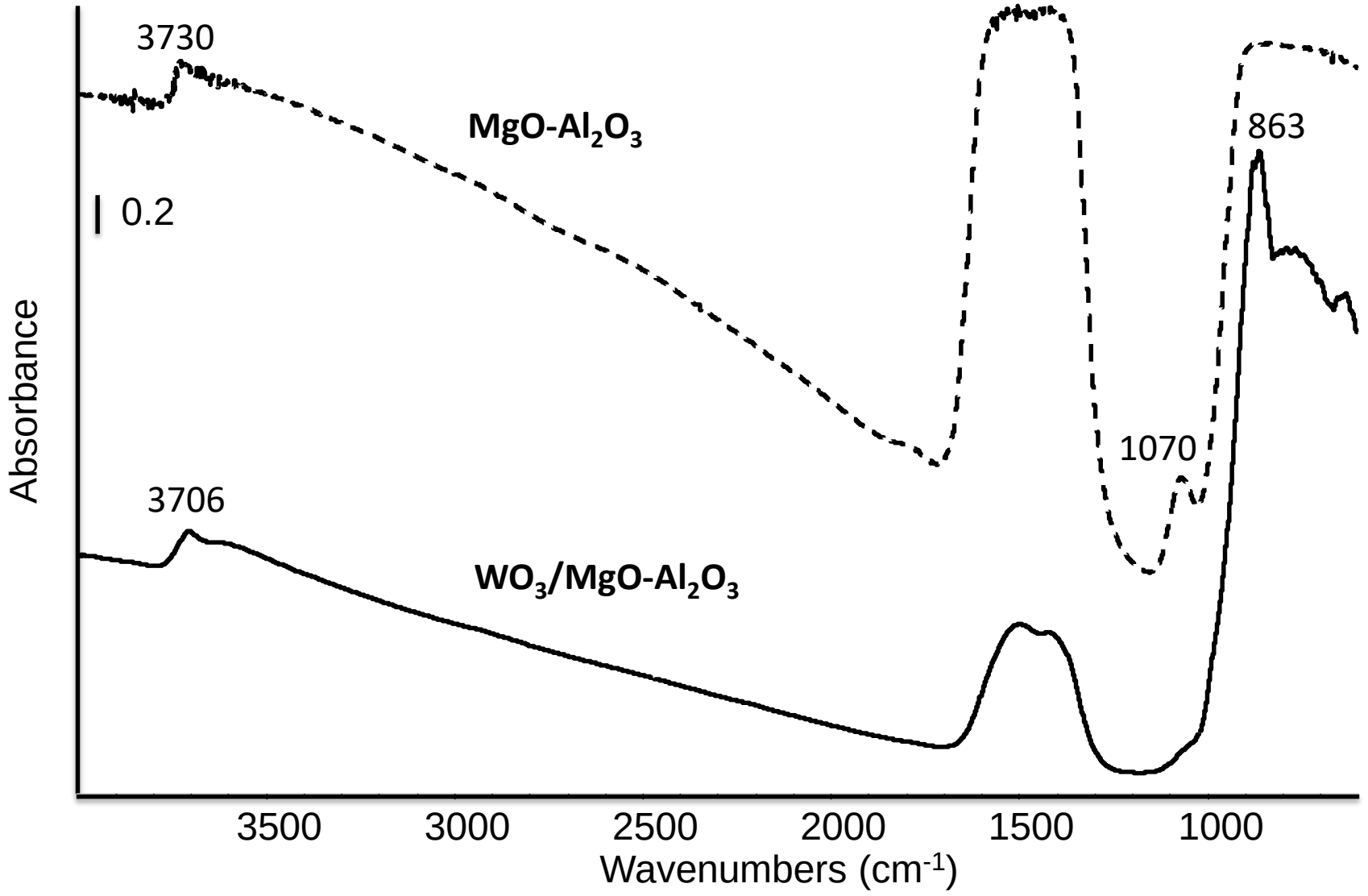
3730
MgO-Al2O3
0.2
Absorbance
863
1070
3706
WO3/MgO-Al2O3
3500
3000
2500
2000
1500
1000
Wavenumbers (cm-1)

Figure 4. Subtraction spectra- Pyridine at 323 K

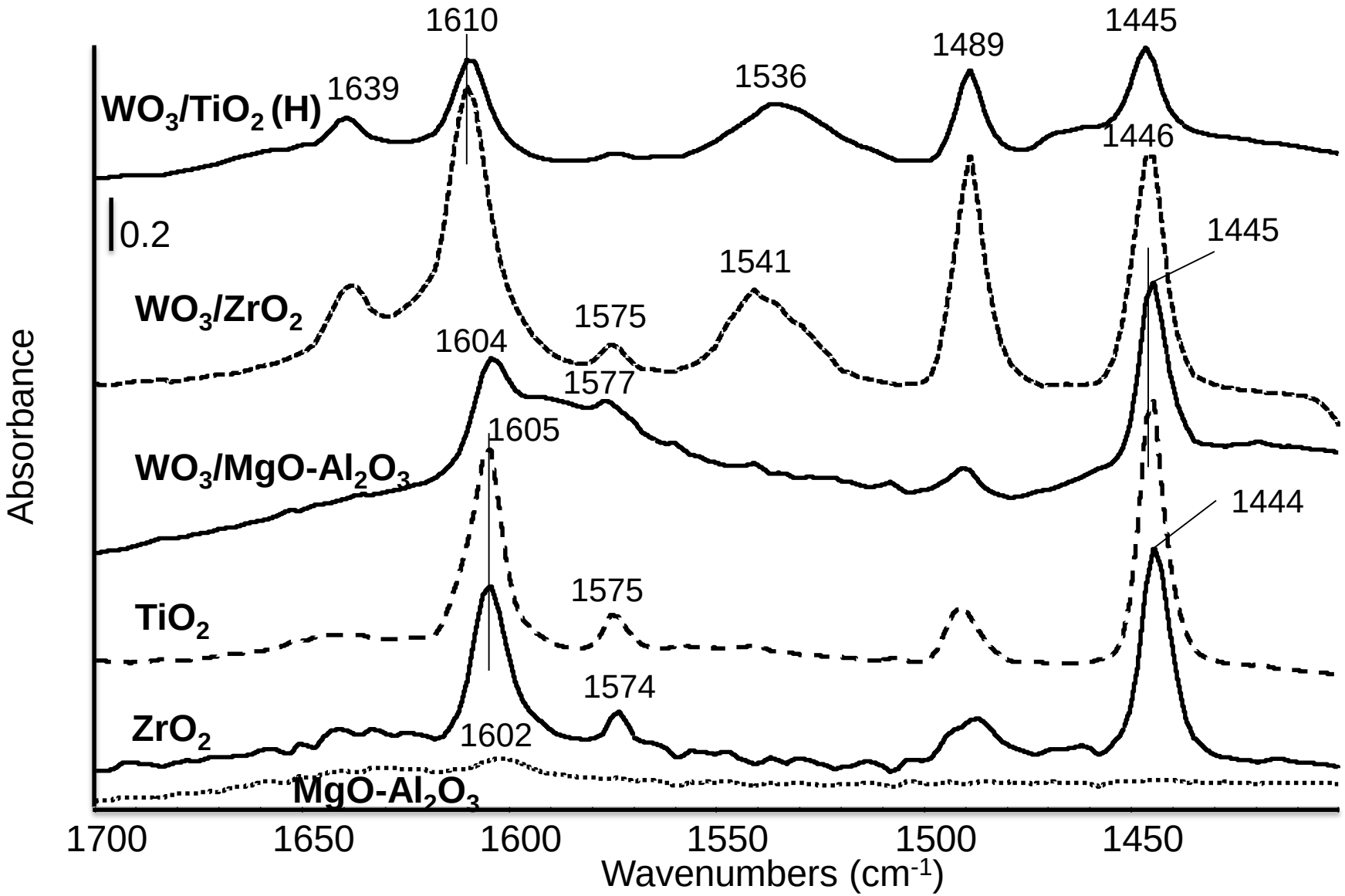

Figure 5.

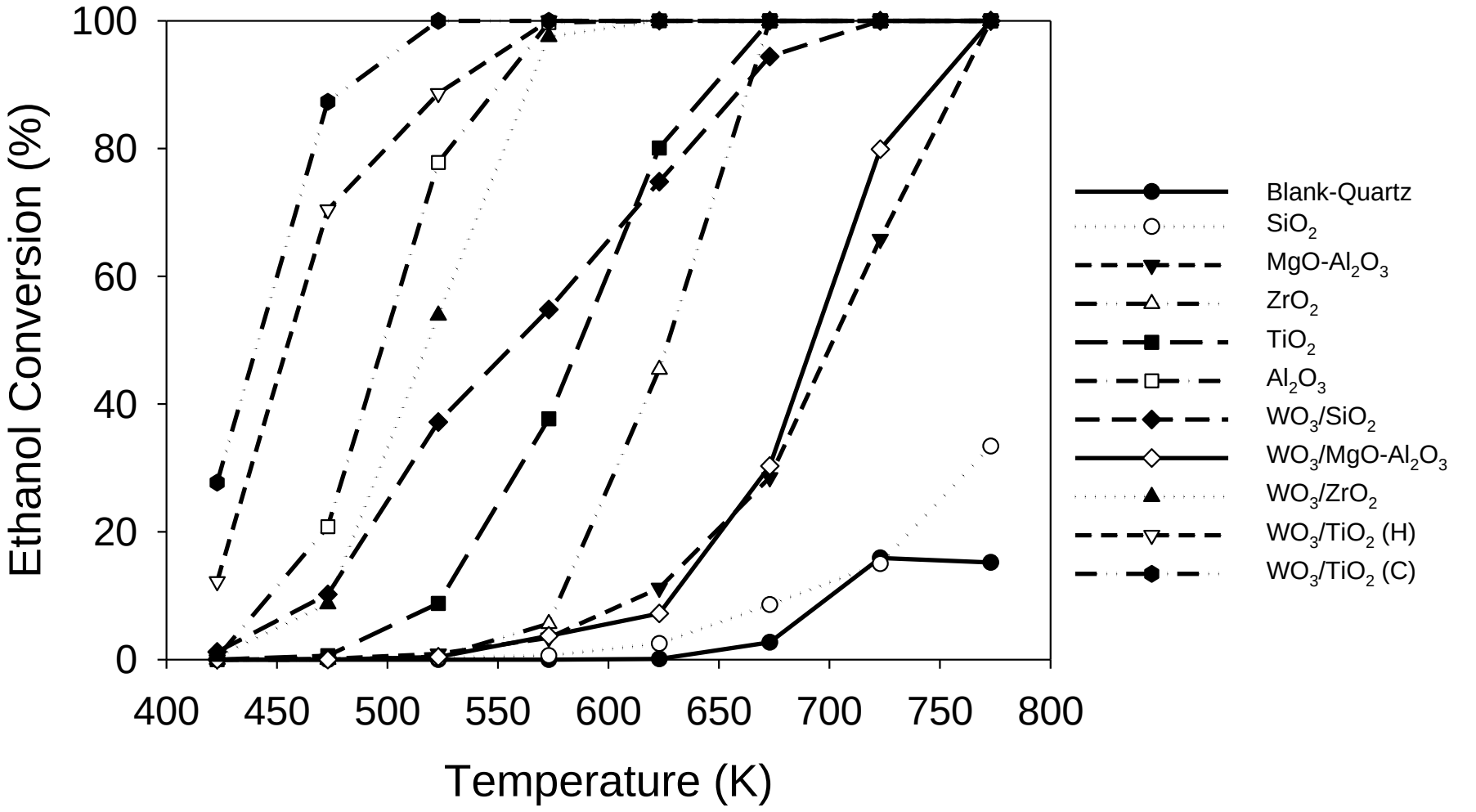
Ethanol Conversion (%)
100
80
60
40
20
0
400
450
500
550
600
650
700
750
800
Temperature (K)
Blank-Quartz
SiO2
MgO-Al2O3
ZrO2
TiO2
Al2O3
WO3/SiO2
WO3/MgO-Al2O3
WO3/ZrO2
WO3/TiO2 (H)
WO3/TiO2 (C)

Figure 6.

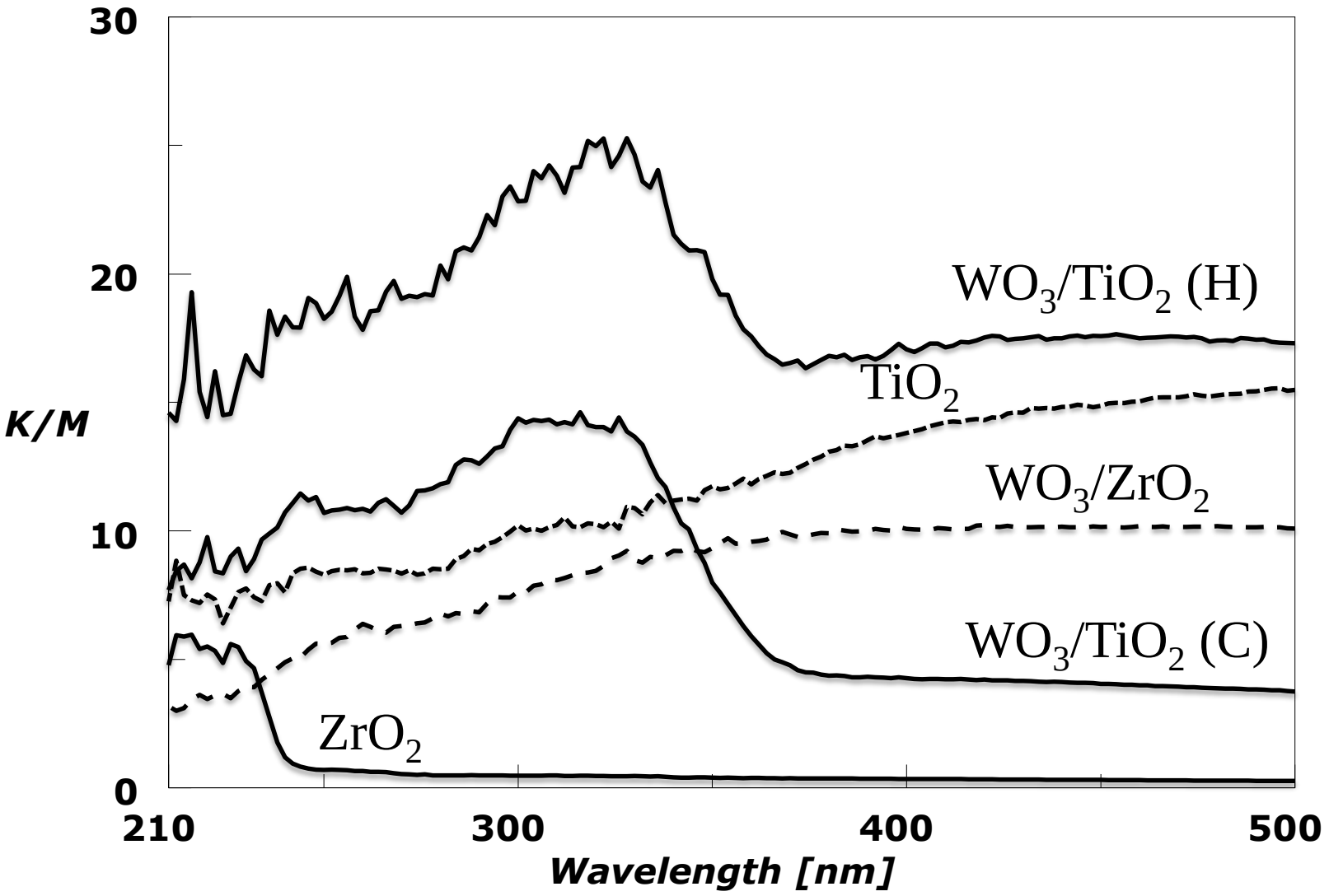
30
20
10
0
K/M
210
300
400
500
Wavelength [nm]
WO3/TiO2 (H)
TiO2
WO3/ZrO2
WO3/TiO2 (C)
ZrO2